*Fluid Dynamics & Materials Processing*
DOI:10.32604/fdmp.2020.010722
***Article***

# An Experimental Study on the Pressure Distribution in Horizontal Gas Wells

**Jinbo Liu[1], Ziheng Jiang[2], Xuezhang Feng[1], Ruiquan Liao[2], Dianfang Feng[1], Xingkai Zhang[2,*] and Hasimu Aikeremu[1]**

[1]No. 1 Gas Production Plant of Xinjiang Oilfield Company, Karamay, 834000, China
[2]School of Petroleum Engineering, Yangtze University, Wuhan, 430100, China
[*]Corresponding Author: Xingkai Zhang. zhangxingkai001@163.com
Received: 23 March 2020; Accepted: 24 September 2020

**Abstract:** Laboratory experiments have been carried out to study the fluid flow in the wellbore of a horizontal gas well during the production process. The related pressure distribution has been determined considering different cases (different inflow media, different perforation opening methods and different liquid holdup). It has been found that the larger the fluid flow rate, the greater the pressure changes in the wellbore under the same hole opening mode. The uniformity of the perforation opening method was also an important factor affecting the magnitude of the wellbore pressure change. The liquid holdup also affected the pressure distribution, especially when the gas volumetric flow rate exceeded 200 $m^3/h$. Comparison of the outcomes of the present experimental study with the predictions of a theoretical model available in the literature has provided a relative error smaller than 20%.

**Keywords:** Horizontal gas well; laboratory experiment; pressure distribution

**Nomenclature**

| | |
|---|---|
| $p_w$: | pressure along horizontal well (Pa) |
| $n$: | number of perforations |
| $q_w$: | well rate at arbitrary position along horizontal well (m/s) |
| $L$: | perforation length (m) |
| $v_p$: | fluid velocity in perforation (m/s) |
| $R_w$: | flow resistivity inside horizontal well |
| $d$: | bore diameter (m) |
| $x$: | coordinate along horizontal well |
| $D$: | inner diameter of borehole unit (m) |
| $\alpha$: | parameter in description of turbulent flow |
| $\tau_w$: | wall shear stress ($N/m^2$) |
| $F_{mix}$: | mixed pressure drop (Pa) |
| $\Delta p$: | pressure drop (Pa) |
| $A$: | cross section of fluid flow ($m^2$) |
| $R$: | injection ratio |
| $f$: | friction coefficient |

$\rho$: density (Kg/m$^3$)
$v_m$: mixing velocity (m/s)
$v_1$: velocity at upstream end (m/s)
$\rho_m$: mixing density (Kg/m$^3$).

## 1 Introduction

With the reform of China's energy structure and the increasing demand for natural gas, shale gas as a clean energy has become an important supplement to promote sustainable social development [1]. Horizontal wells can expand the open-hole area of the reservoir. For this reason, it has a significant effect on improving oil and gas recovery and oil as well as gas production in a single well. Horizontal well technology is targeted at thin oil and gas reservoirs, which can greatly increase single well production, and its application in oil and gas fields is very prominent [2]. Due to the seepage of the fluid in the reservoir near the well, there is a constant flow of fluid from the well wall to the wellbore along the horizontal well. The multiphase flow in wellbore reservoir is mainly controlled by the fluid pressure along the wellbore, and is related to the reservoir deformation during completion and oil and gas production. In the process of oil and gas exploitation, 60%–80% of energy loss is in the wellbore [3]. However, the fluid pressure in the wellbore depends on the flow state of multiphase flow in the pipe, wellhead control conditions and the seepage flow of multiphase fluid in the reservoir also affects the flow in the horizontal well [4,5]. We can use the measured pressure to estimate reservoir characteristics through logging analysis during transient flow [6]. Therefore, in-depth study of the pressure distribution in the wellbore is of great significance to the analysis of oil and gas reservoir productivity and optimization of production technology.

In 1989, Dikken [7] proposed that the pressure drop in the wellbore should not be ignored, and deduced the expression of the friction pressure drop on the pipe wall as follows:

$$\frac{d}{dx}p_w(x) = R_w q_w(x)^{2-\alpha} \tag{1}$$

In 1990, Islam [8] conducted a series of experiments to simulate the fluid flow in horizontal wells. The results showed that the flow in the wellbore was quite different from the typical pipe flow due to the perforation of horizontal wells. In 1994, Su [9] derived the mathematical model of pressure drop of single, two and three holes, and then obtained the mathematical model of pressure drop of perforated horizontal well. He concluded that the total pressure drop of horizontal wellbore is mainly composed of acceleration pressure drop, wall friction, perforation roughness and mixed effect. In 1996, Ouyang [10] studied single-phase and two-phase flow in horizontal wellbore. In the range of parameters set in the experiment, the resistance coefficients of the wellbore under laminar flow and turbulent flow were discussed, and the resistance coefficients of the production wellbore were summarized. It was found that in the laminar flow condition, the wall inflow increased the resistance coefficient, while in the turbulent flow condition, the wall inflow reduced the resistance coefficient. From 1998 to 2000, Zhou et al. [11,12] designed a variable-mass flow simulation device for horizontal wells, which was applied to the simulation of the single-hole inflow of the water medium in the horizontal well. In the simulation process, the pressure drop along the pipeline was divided into three parts: friction pressure drop, acceleration pressure drop and mixed pressure drop. In 2011, Wang et al. [13] studied the relationship between the inflow of wall orifices and the main flow pressure drop in the pipe through the indoor loop test. With the increase of injection ratio, the pressure drop in the tube increased. Due to the interaction between the inflow and the main flow, an additional pressure drop was recorded wose value was linear with the ratio of acceleration pressure drop and injection ratio. For different injection ratio conditions, the total pressure

drop of wellbore was divided into the sum of friction pressure drop and additional pressure drop of perforating pipe, and the w-w-x model was established:

$$\Delta p_{total} = \Delta p_{wall} + \Delta p_{add} \tag{2}$$

$$\Delta p_{add} = \begin{cases} 4.0703\Delta p_{acc}/R(0 < R \leq 2) \\ 6.3371\Delta p_{acc}/R(2 < R \leq 20) \\ 10.7520\Delta p_{acc}/R(R = 20) \end{cases} \tag{3}$$

In 2013, Wei et al. [14] studied the effects of perforation parameters and cavity injection on frictional pressure drop, accelerated pressure drop, and mixed pressure drop of horizontal wellbore walls through single-phase flow experiments. In 2015, Wang [1] conducted numerical simulation research on single, two- and three-holes models, and proposed a pressure drop estimation model:

$$\Delta p = \rho {v_1}^2 (2nL\frac{v_p 2}{v_1}\frac{d^2}{D^2} + n^2L^2\frac{{v_p}^2}{{v_1}^2}\frac{d^4}{D^4}) + \tau_w\frac{L}{D} + \frac{F_{mix}}{A} \tag{4}$$

In 2016, Zhao [15] studied variable density perforating horizontal well technology, combining the interaction with formation fluid and wellbore fluid through the theoretical knowledge of percolation and fluid mechanics, combined with the interactions of formation fluids and wellbore fluids, the reservoir percolation model and wellbore wall inflow model and wellbore internal pressure were then derived. In 2018, Wen [16] studied the single-phase variable mass flow of perforation-free horizontal pipe, single-hole horizontal pipe and double-hole horizontal pipe, and proposed the friction coefficient expression of perforation-free horizontal pipe by fitting the experimental data.

From the discussion, it appears there is no in-depth discussion on the multi-perforation and multi-perforation cluster in the previous researches. Therefore, it is of great significance to carry out the experimental research and theoretical analysis on multi-perforation horizontal wellbores for the horizontal wellbore mining process.

## 2 Experimental Perforated Horizontal Wellbore Device and System

A schematic diagram of the horizontal gas well gas-liquid two-phase simulation experiment system is shown in Fig. 1 [17]. A photo of the field experimental device is shown in Fig. 2. The device includes a water pump, a compressor, a water flow device connected to the water pump outlet, and a gas flow device connected to the compressor outlet. Gas and liquid flow rate are controlled by water pump and air compressor respectively. The outlet of the gas-liquid distributor is in communication with the main inlet gas-liquid mixer and each cluster perforation inlet front mixer, and a flow meter is arranged on its communication pipeline. Each cluster of perforations contains six perforations, and the incoming flow can be transported to each hole through the mixer. Each perforation can be adjusted through a switching valve, and different perforation clusters can be obtained by changing different perforation clusters to simulate the effect of different perforation parameters on the gas-liquid two-phase flow.

The length of the experimental pipe section is 10 m the set-up can be regarded as intercepting some pipe sections in the actual production situation and will prove useful for analysis and research. Through this experiment, the pressure distribution in the wellbore can also be investigated.

The device is equipped with a total of 14 pressure sensors, which can measure the pressure distribution in the wellbore, and can also monitor the pressure at the mainstream inlet and perforation clusters. The arrangement of each pressure collection point is shown in Tab. 1 below.

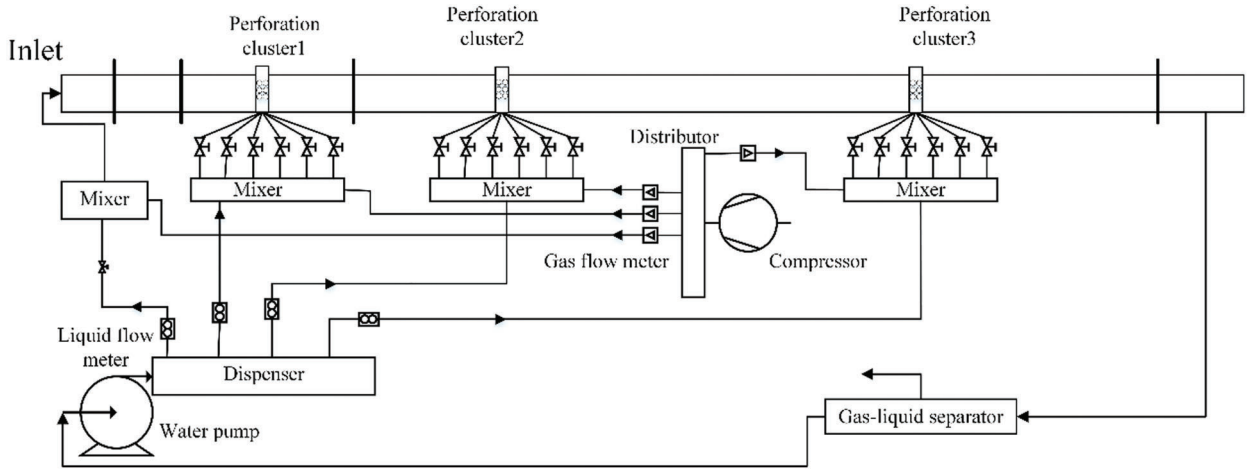


**Figure 1:** Two-phase simulation experiment system for horizontal gas wellbore [17]

**Figure 2:** Experimental device diagram [17]

**Table 1:** Arrangement of pressure measuring points

| Acquisition point No. | Distance from the inlet (m) | Physical position | Acquisition point No. | Distance from the inlet (m) | Physical position |
|---|---|---|---|---|---|
| 1 | 0 | Behind the main inlet valve | 8 | 2.79 | Downstream of the inlet of the second perforation cluster |
| 2 | 0.96 | Upstream of the first perforation cluster | 9 | 2.83 | Downstream of the second perforation cluster |
| 3 | 1.05 | Upstream of the first perforation cluster inlet | 10 | 5 | Measuring points between two and three clusters |
| 4 | 1.25 | Downstream of the first perforation cluster inlet | 11 | 5.87 | Upstream of the third perforation cluster |

**Table 1 (continued).**

| Acquisition point No. | Distance from the inlet (m) | Physical position | Acquisition point No. | Distance from the inlet (m) | Physical position |
|---|---|---|---|---|---|
| 5 | 1.29 | Downstream of the first perforation cluster | 12 | 5.96 | Upstream of the inlet of the third perforation cluster |
| 6 | 2.37 | Upstream of the second perforation cluster | 13 | 6.29 | Downstream of the inlet of the third perforation cluster |
| 7 | 2.46 | Upstream of the entrance of the second perforation cluster | 14 | 6.33 | Downstream of the third perforation cluster |

There are three perforating clusters in the device, the distance between the two clusters increases gradually, forming a variable density perforating pipeline, and the distribution of pressure measuring points is uneven with the density of perforating clusters.

## 3 Experimental Results and Analysis

### *3.1 Results and Analysis of Single-Phase Gas Experiments*

#### *3.1.1 Pressure Distribution in Wellbore*

First, in the case of single-phase gas, the mode of opening is (0,2,0), that is, the first perforation cluster opens 0 holes, the second perforation cluster opens 2 holes, and the third perforation cluster opens 0 holes. The pressure distribution under different air intake conditions is obtained, as shown in Fig. 3. It can be seen from the figure that there will be a period of pressure drop from the main inlet to the upstream of the first cluster of perforating inlet, and then the drop will start to slow down. From the upstream of the first cluster to the downstream of the first cluster, the pressure tends to increase obviously, which may be due to the large fluctuation of the fluid in the tube caused by the mixing of the fluid in the second cluster, shown as the increase of the pressure in the first cluster of perforations. The area with the largest pressure change range is from the upstream of the second cluster to the downstream of the second cluster, and then the pressure change of the whole pipeline is no longer obvious. When perforating into the flow, the gas flows through the perforating first, and its aperture is small, which has a compression effect on the gas. When the gas enters the wellbore, it will cause a sharp increase in the pressure. Later, because the fluid flows into the large aperture from the small aperture, the gas diffusion will cause a sharp decrease in the pressure. Moreover, with the increase of perforating air intake, the pressure near the perforating cluster also increases, and the value of pressure increase is about 0.2 MPa for every 50 $m^3/h$ gas volume increase.

In addition, in the process of fluid flowing from the downstream of the second perforating cluster to the third perforating cluster, the perforating gas will have a certain impact on the mixed fluid in the wellbore and cause the pressure change in the wellbore due to the continuous inflow of the wellbore inlet and the second perforating cluster.

Tab. 2 shows the changes in pressure distribution in the wellbore when opening (1,1,1), (2,2,2), (3,3,3) and (4,4,4).

Tab. 2 shows the changes in the pressure distribution in the wellbore when opening (1,1,1), (2,2,2), (3,3,3) and (4,4,4). It can be seen that when the number of perforations is (1,1,1), the pressure in the wellbore will change significantly with the change of perforations. Unlike Fig. 3, when all three clusters

of perforations begin to feed, there is a significant change in pressure in the wellbore near each cluster of perforations. The larger the gas volume is, the greater the pressure in the wellbore will be. Because of the same amount of air in each perforation under different conditions, the increasing range of the pressure at the perforation is basically the same under the same amount of air intake; the changing trend of the pressure in the whole wellbore under different conditions is also the same.

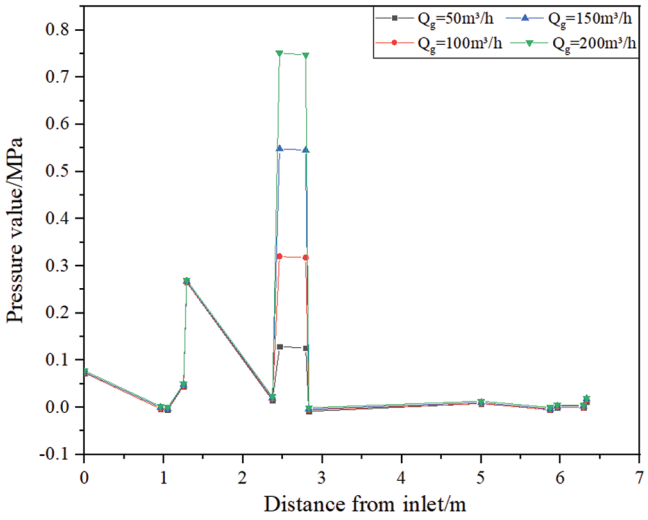


**Figure 3:** Distribution of wellbore pressure during perforation (0,2,0)

**Table 2:** Pressure data for opening (1,1,1), (2,2,2), (3,3) and (4,4,4)

| Opening model | (1,1,1)/m³d$^{-1}$ | | | (2,2,2)/m³d$^{-1}$ | | | (3,3,3)/m³d$^{-1}$ | | | (4,4,4)/m³d$^{-1}$ | | |
|---|---|---|---|---|---|---|---|---|---|---|---|---|
| Pressure/MPa<br>Distance from inlet/m | 200 | 300 | 500 | 200 | 300 | 500 | 200 | 300 | 500 | 200 | 300 | 500 |
| 0 | 0.46 | 0.68 | 1.06 | 0.44 | 0.63 | 0.95 | 0.50 | 0.71 | 1.12 | 0.51 | 0.67 | 1.10 |
| 0.96 | 0.39 | 0.61 | 0.99 | 0.37 | 0.56 | 0.88 | 0.43 | 0.64 | 1.05 | 0.44 | 0.60 | 1.03 |
| 1.05 | 0.59 | 0.91 | 1.81 | 0.42 | 0.64 | 1.01 | 0.45 | 0.66 | 1.10 | 0.45 | 0.61 | 1.06 |
| 1.25 | 0.44 | 0.66 | 1.04 | 0.48 | 0.69 | 1.06 | 0.51 | 0.72 | 1.16 | 0.51 | 0.67 | 1.12 |
| 1.29 | 0.58 | 0.80 | 1.18 | 0.56 | 0.75 | 1.07 | 0.62 | 0.83 | 1.24 | 0.63 | 0.79 | 1.23 |
| 2.37 | 0.42 | 0.67 | 1.02 | 0.40 | 0.59 | 0.87 | 0.47 | 0.67 | 1.08 | 0.48 | 0.64 | 1.07 |
| 2.46 | 0.59 | 0.94 | 1.82 | 0.42 | 0.64 | 0.97 | 0.45 | 0.67 | 1.10 | 0.45 | 0.61 | 1.06 |
| 2.79 | 0.38 | 0.60 | 0.98 | 0.42 | 0.64 | 1.01 | 0.45 | 0.67 | 1.10 | 0.45 | 0.61 | 1.06 |
| 2.83 | 0.38 | 0.63 | 0.98 | 0.36 | 0.55 | 0.84 | 0.43 | 0.63 | 1.05 | 0.43 | 0.59 | 1.03 |
| 5 | 0.40 | 0.65 | 1.00 | 0.38 | 0.57 | 0.86 | 0.45 | 0.65 | 1.07 | 0.46 | 0.62 | 1.05 |
| 5.87 | 0.38 | 0.63 | 0.98 | 0.36 | 0.55 | 0.84 | 0.43 | 0.63 | 1.05 | 0.44 | 0.60 | 1.03 |
| 5.96 | 0.59 | 0.94 | 1.82 | 0.42 | 0.64 | 0.97 | 0.45 | 0.66 | 1.10 | 0.45 | 0.61 | 1.06 |
| 6.29 | 0.39 | 0.64 | 0.99 | 0.43 | 0.65 | 0.98 | 0.46 | 0.68 | 1.11 | 0.46 | 0.62 | 1.07 |
| 6.33 | 0.39 | 0.63 | 0.99 | 0.38 | 0.58 | 0.88 | 0.43 | 0.64 | 1.05 | 0.44 | 0.60 | 1.04 |

When the first perforation cluster is in charge, the pressure increases from the upstream to the downstream of the first cluster. When the gas volume increases to a certain extent, there is a pressure drop between the downstream of the first cluster perforation and the downstream of the first cluster barrel. In the second cluster and the third cluster perforation, the pressure first increases, then stabilizes and then decreases. Compared with the opening (1,1,1), when the opening is (2,2,2), the pressure variation amplitude of the perforated section is reduced. Because in each perforation section, the number of perforations increases, and the biggest difference with the case of single hole opening is that under the condition of porous opening, because the perforations are circumferentially distributed, the phase angle is 60°, when two holes flow in at the same time, there will be a mutual impact between perforations, and this force is to reduce the impact of pressure change intensity caused by perforations.

The distribution trend of wellbore pressure is the same when opening hole (3,3,3), (4,4,4) and opening hole (2,2,2). Similarly, due to the influence of wellbore friction from the wellbore inlet to the upstream of perforation, the fluid will produce a certain pressure drop in the flow process after entering the wellbore, and the mass flow of mixed fluid in the wellbore will increase when perforating air enters, and the pressure will start to decrease after leaving the perforating section. In addition, there is a certain difference in the pressure change between the first perforation cluster and the other two clusters, mainly because the distance between the downstream of the first perforation cluster and the upstream of the second perforation cluster is 1 m, and the inflow of the second perforation cluster will cause the local return flow of the pipeline. When there are multiple perforations at the same time, the divergence degree of air in the pipeline will increase, which will cause the pressure of the first perforation segment to show a holding the trend of continuous rise.

### *3.1.2 Effect of Perforation Opening Method on Pressure Distribution in Wellbore*

Fig. 4 compares the pressure distribution in the wellbore under the conditions of hole opening (0,2,0), (0,2,2), (2,2,0), (1,1,1), (2,2,2), (3,3,3) and (4,4,4) with air intake of 200 m³/h. Among the 7 kinds of opening conditions, the last four are relatively uniform. It can be found that compared with non-uniform densities, the overall pressure change amplitude is smaller and the trend is obvious.

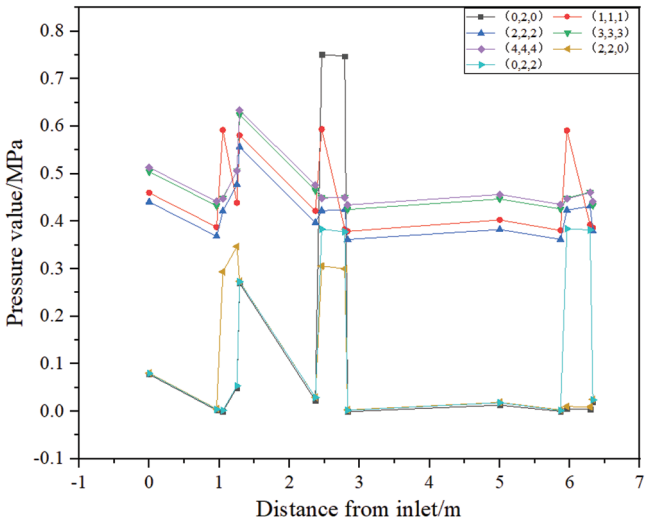


**Figure 4:** Wellbore pressure distribution with different perforation methods with air intake of 200 m³/h

Fig. 5 shows the pressure distribution in the wellbore when the number of perforations in each segment is irregular. It can be found that when the number of perforations is small, the pressure near the perforations in

the wellbore changes greatly. For example, when the number of perforations increases from (1,2,1) to (1,6,1), the pressure peak near the perforations decreases, indicating that the single cluster change of the second cluster of perforations will affect the pressure distribution of other components in the wellbore; by comparing (1,2,3), (2,4,6), (3,4,5) and (4,3,2), it can be found that with the increase of perforation number, the change of wellbore pressure tends to be stable. In other areas of the wellbore, the effect of 200 $m^3$/h air intake on the pressure in the wellbore is not obvious.

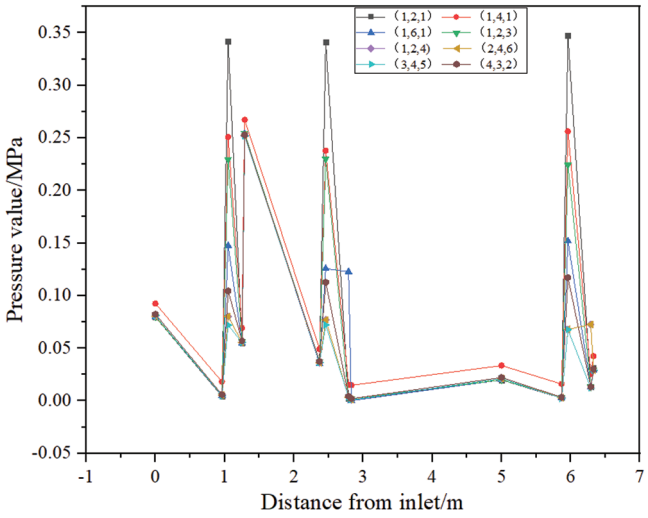


**Figure 5:** Wellbore pressure distribution of 200 $m^3$/h air intake with different opening methods

### *3.2 Gas-liquid Two-Phase Experiment Results and Analysis*

#### *3.2.1 Effect of Liquid Volume on Pressure Distribution in Wellbore*

Fig. 6 shows that the perforation air intake is maintained at 50 $Vm^3$/h when the perforation method is (0,2,0). The pressure distribution in the wellbore obtained by continuously changing the perforation flow rate. It can be clearly found that after increasing a certain amount of fluid, the pressure in the wellbore as a whole is increasing. This is because in addition to the inflow of gas, liquid also enters the wellbore. At this time, the wellbore is a variable mass of the flow state. The increase in the mass of fluid in the wellbore caused by fluid flow through the wellbore at various points of pressure, the higher the elevation and the more the fluid volume increases, the greater the increase in pressure in the wellbore and the more pronounced the increase in pressure near the perforation.

Compared with the gas volume of 50 $m^3$/h, when the gas volume is 100 $m^3$/h, the pressure near the second perforated cluster increases to about 0.7 MPa, which is 0.2 MPa higher than the pressure of the perforated cluster at 0.6 $m^3$/h in Fig. 7. In the vicinity of the first perforation cluster, although there is no fluid in the perforation, the pressure of the perforation cluster still fluctuates due to the influence of the second perforation cluster. The pressure is not greatly affected by the amount of fluid.

Tab. 3 shows the pressure distribution in the wellbore with different liquid volume under the opening mode (2,2,2), gas volume of 200 $m^3$/h, 300 $m^3$/h, 500 $m^3$/h and 600 $m^3$/h.

When all three perforating clusters open, there will be three places where the pressure changes violently. Similarly, the pressure of each point in the wellbore will increase as a whole when the perforating fluid inflow is increased. The larger the liquid volume is, the greater the pressure of each point in the wellbore is. Comparing the data in the table, it can be found that when the gas volume increases to 300 $m^3$/h, 500 $m^3$/h and 600 $m^3$/h, the pressure changes under four different liquid volumes are very obvious, and the trend of pressure changes is

the same. Especially, from the downstream of the second perforation cluster barrel to the upstream of the third perforation cluster barrel, the pressure first increases and then decreases. The turning point occurs at the measuring point between the second cluster and the third cluster, that is, 5 m away from the inlet.

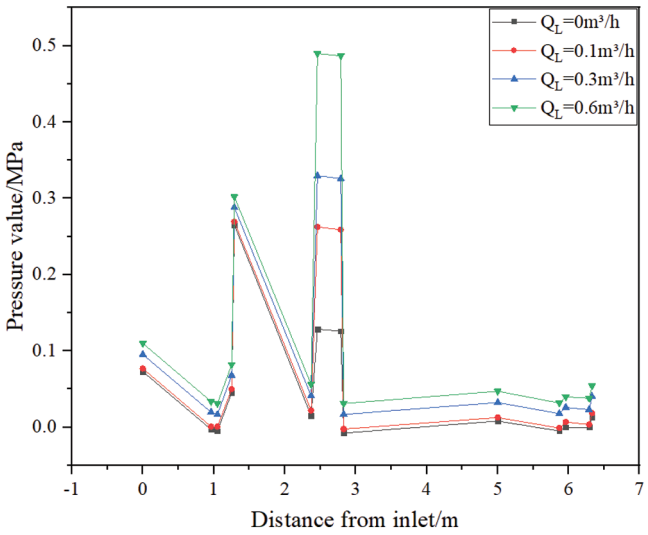


**Figure 6:** Pressure distribution in the wellbore under the conditions of different fluid volume when the hole volume is (0,2,0)

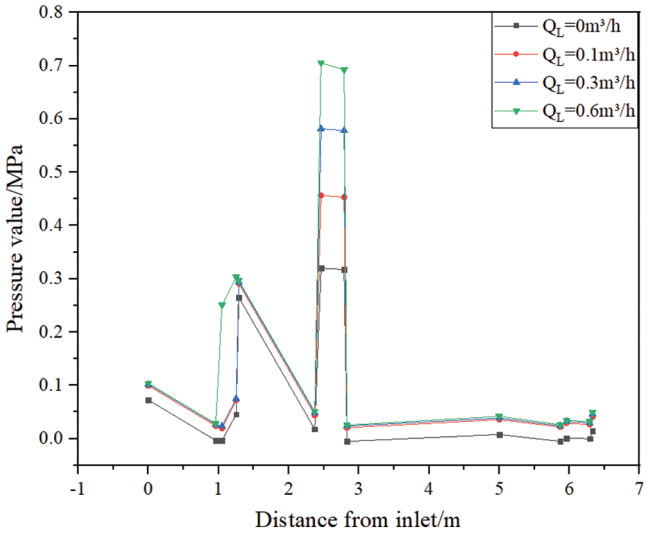


**Figure 7:** Pressure distribution in the wellbore with open holes (0,2,0) and gas volume of 100 m³/h

*3.2.2 Effect of Fluid Accumulation on Pressure Distribution in Wellbore*

Figs. 8–11 record the distribution of pressure in the wellbore when different gas volumes are injected into the perforations under different liquid holdup conditions. It can be found that when there is effusion in the wellbore, the variation trend of pressure in the wellbore is the same as that in the case of no holdup rate in Fig. 8. By comparing Figs. 8 and 9, it can be found that a small amount of effusion will cause an increase in the pressure near the perforation. By comparing Figs. 9 and 10, it can be found that with the increase of fluid accumulation in the wellbore, the pressure at the perforation will decrease, because when the fluid

accumulation increases to a certain extent, the gas phase distribution volume in the pipeline significantly decreases, and the velocity at the perforation varies greatly, resulting in an increase of acceleration pressure drop. At the same time, when the gas volume is greater than 200 $m^3/h$, the pressure in the wellbore will increase due to the change of the two-phase flow pattern in the wellbore. Therefore, in the case of different liquid holdup, there will be a pressure drop near the perforation. When the air intake volume of the perforation increases to a certain extent, there is a pressure increase everywhere in the wellbore except the perforation.

**Table 3:** Pressure data of different gas-liquid volume under opening (2,2,2)

| Opening model | 200/$m^3h^{-1}$ | | | 300/$m^3h^{-1}$ | | | 500/$m^3h^{-1}$ | | | 600/$m^3h^{-1}$ | | |
|---|---|---|---|---|---|---|---|---|---|---|---|---|
| Pressure/MPa | Liquid volume/$m^3h^{-1}$ | | | | | | | | | | | |
| Distance from inlet/m | 0.1 | 0.3 | 0.6 | 0.1 | 0.3 | 0.6 | 0.1 | 0.3 | 0.6 | 0.1 | 0.3 | 0.6 |
| 0 | 0.43 | 0.52 | 0.57 | 0.63 | 0.71 | 0.89 | 1.05 | 1.24 | 1.37 | 1.25 | 1.48 | 1.55 |
| 0.96 | 0.36 | 0.45 | 0.50 | 0.56 | 0.64 | 0.82 | 0.97 | 1.17 | 1.30 | 1.18 | 1.41 | 1.48 |
| 1.05 | 0.43 | 0.56 | 0.68 | 0.66 | 0.77 | 1.00 | 1.14 | 1.39 | 1.56 | 1.37 | 1.67 | 1.75 |
| 1.25 | 0.49 | 0.62 | 0.74 | 0.72 | 0.83 | 1.06 | 1.19 | 1.45 | 1.62 | 1.43 | 1.73 | 1.81 |
| 1.29 | 0.55 | 0.64 | 0.69 | 0.75 | 0.83 | 1.01 | 1.16 | 1.36 | 1.49 | 1.37 | 1.60 | 1.67 |
| 2.37 | 0.39 | 0.48 | 0.53 | 0.59 | 0.66 | 0.85 | 1.00 | 1.19 | 1.33 | 1.21 | 1.44 | 1.55 |
| 2.46 | 0.43 | 0.57 | 0.68 | 0.66 | 0.78 | 1.00 | 1.14 | 1.40 | 1.56 | 1.38 | 1.67 | 1.80 |
| 2.79 | 0.43 | 0.57 | 0.68 | 0.66 | 0.78 | 1.00 | 1.14 | 1.40 | 1.56 | 1.38 | 1.67 | 1.75 |
| 2.83 | 0.35 | 0.44 | 0.49 | 0.55 | 0.63 | 0.81 | 0.97 | 1.16 | 1.30 | 1.18 | 1.40 | 1.51 |
| 5 | 0.37 | 0.46 | 0.51 | 0.57 | 0.65 | 0.83 | 0.99 | 1.18 | 1.32 | 1.20 | 1.42 | 1.53 |
| 5.87 | 0.35 | 0.44 | 0.49 | 0.55 | 0.63 | 0.81 | 0.97 | 1.16 | 1.30 | 1.18 | 1.40 | 1.51 |
| 5.96 | 0.43 | 0.57 | 0.68 | 0.66 | 0.78 | 1.00 | 1.14 | 1.39 | 1.56 | 1.38 | 1.67 | 1.80 |
| 6.29 | 0.44 | 0.58 | 0.69 | 0.67 | 0.78 | 1.01 | 1.15 | 1.40 | 1.57 | 1.38 | 1.68 | 1.81 |
| 6.33 | 0.36 | 0.45 | 0.50 | 0.56 | 0.64 | 0.82 | 0.98 | 1.17 | 1.31 | 1.19 | 1.42 | 1.52 |

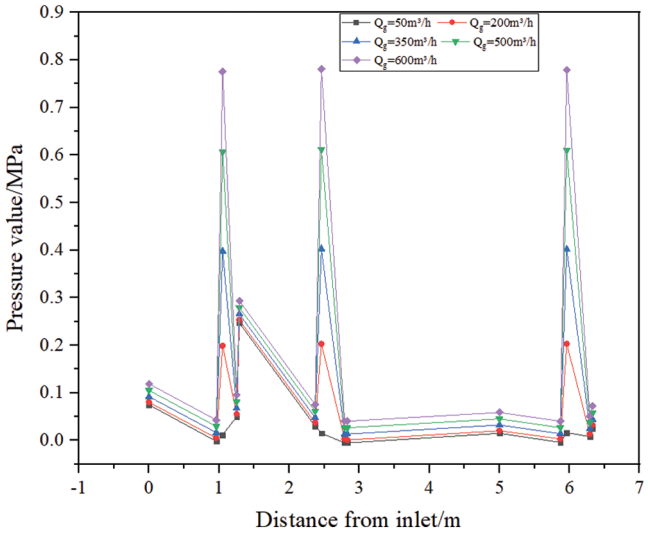


**Figure 8:** Pressure distribution in the wellbore with 0% fluid holding rate and different gas volumes

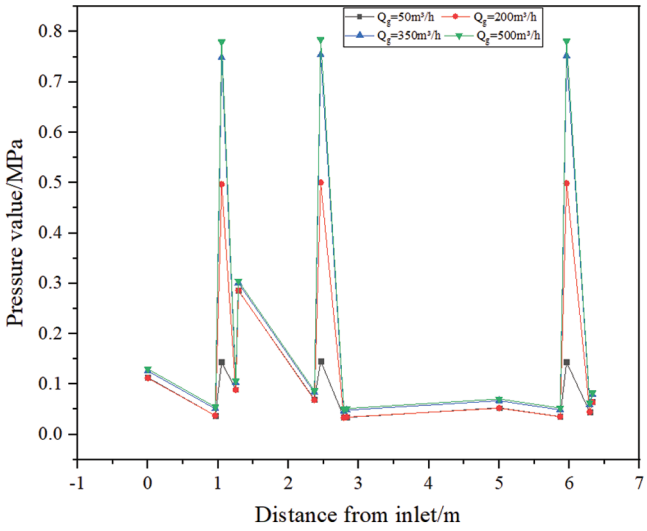


**Figure 9:** Pressure distribution in the wellbore with 25% fluid holdup and different gas volumes

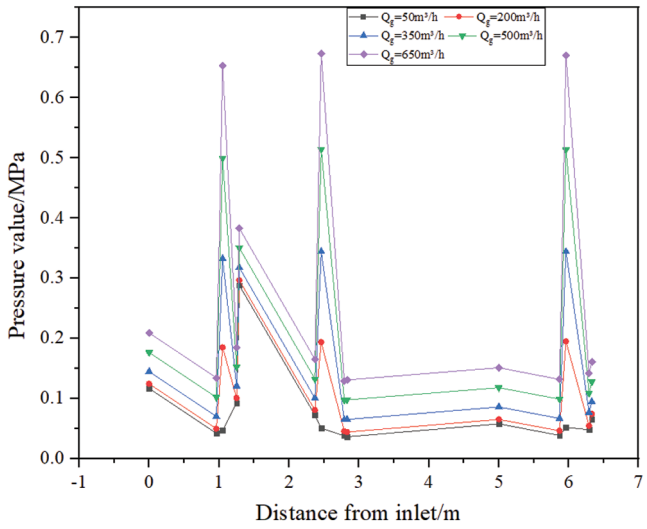


**Figure 10:** Pressure distribution in the wellbore at 50% fluid hold

As can be seen from Fig. 11, after the fluid holding rate in the wellbore exceeds 50%, the perforated air starts to have a strong impact on the fluid accumulation in the wellbore, causing a violent fluctuation of the fluid in the wellbore because of this instability. Compared with the above three figures, the flow of the flow is greatly different. The sudden increase in pressure occurs near the first perforation cluster. At the same time, due to the intake of the first cluster, the pipeline after the first perforation cluster, the fluid in the medium begins to fluctuate greatly, and the liquid directly enters the subsequent perforation or the liquid directly adheres to the pressure sensor. Therefore, the pressure fluctuation and liquid holdup near the second and third perforations are 50% and 50%. The following pressure distributions are different.

*3.2.3 Influence of Intercluster Interference on Pressure Distribution in Gas-Liquid Two-Phase State*

The experiment mainly carried out the test research on the pressure distribution law of inter-cluster interference under three liquid volume conditions of 0.1 $m^3/h$, 0.3 $m^3/h$ and 0.6 $m^3/h$. As shown in Fig. 12, the pressure in the wellbore is the smallest when the first cluster perforation is not injecting

liquid. With the increase of the liquid intake in the second cluster perforation, the pressure everywhere will increase significantly. When the liquid injection volume of the second cluster perforation is increased to 0.6 m³/h, the opening method is (0,2,0), and the pressure near the first perforation section will be higher than the pressure in other test cases. Because the first two clusters of perforations are relatively close, the second cluster of perforations will affect the upstream pressure. As the number of perforation openings increases, the pressure near the perforation clusters decreases, and the overall pressure fluctuation of the wellbore becomes smaller.

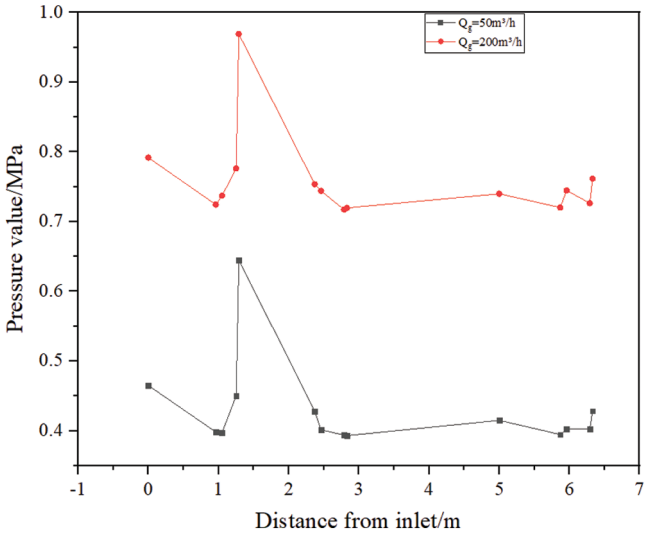


**Figure 11:** Pressure distribution in the wellbore with 75% fluid holdup

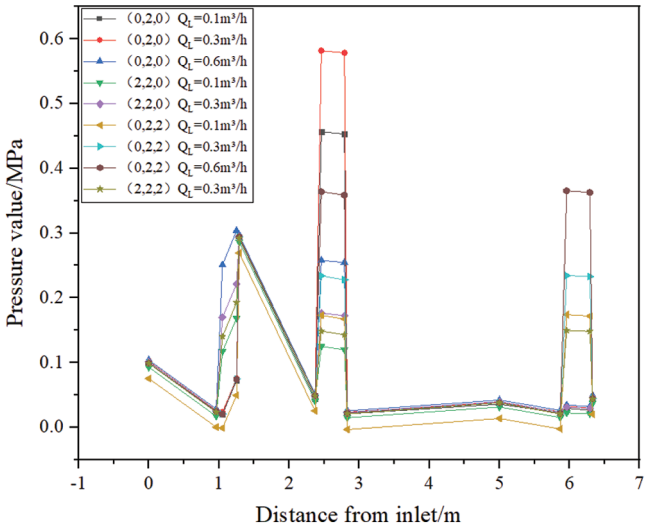


**Figure 12:** Pressure distribution in the wellbore with gas volume of 100 m³/h

Fig. 13 shows the pressure distribution in the wellbore at different liquid volumes when the gas volume is 200 m³/h. Compared with Fig. 12, it can be found that after the gas volume is increased to 200 m³/h, the pressure in the wellbore is more affected by the uniformity of the perforation openings. When the opening

method is (2,2,2), the pressure in the wellbore is higher than that in the non-uniform opening method. As the fluid volume increases, the pressure in the wellbore will increase.

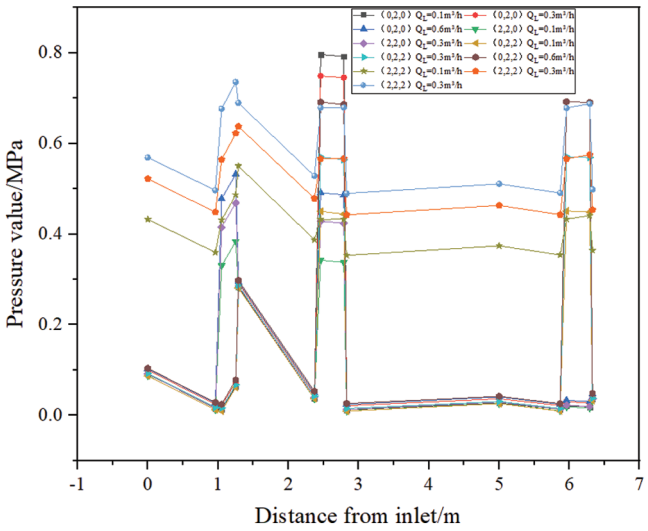


**Figure 13:** Pressure distribution in wellbore with gas volume of 200 m³/h and different fluid volumes

With reference to Figs. 12–14, it can be found that when the gas volume in the wellbore increases to a certain value, the uniformity of the perforation distribution will have a more obvious effect on the pressure in the wellbore. The effect of the change in gas volume on the pressure in the uniform opening mode is greater than that in the non-uniform opening mode. The distance between the first perforation cluster and the main entrance and the second perforation cluster are relatively short. The pressure in the perforation section is affected by the mixture of the two. Whether the first cluster perforation has fluid in it or not, it is near the perforation wall. There will be a pressure rise process everywhere, and after leaving the perforation section, a large pressure drop will be generated under the influence of the second perforation cluster. The difference from the upstream perforation cluster is the third perforation section at the downstream. The pressure of the perforation section will only change significantly when the perforation has inflow. The distance from the inlet has a great influence on the pressure distribution in the wellbore.

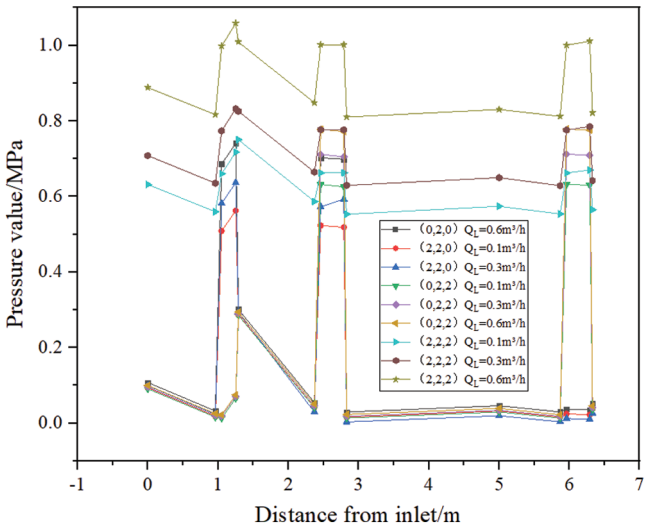


**Figure 14:** Pressure distribution in wellbore with gas volume of 300 m³/h and different fluid volumes

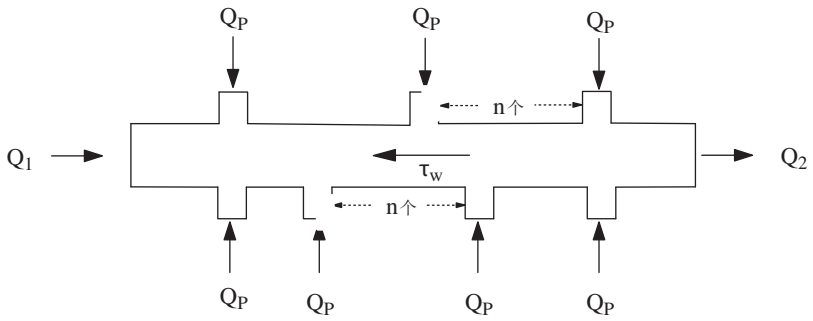


**Figure 15:** Multi-perforation inflow model

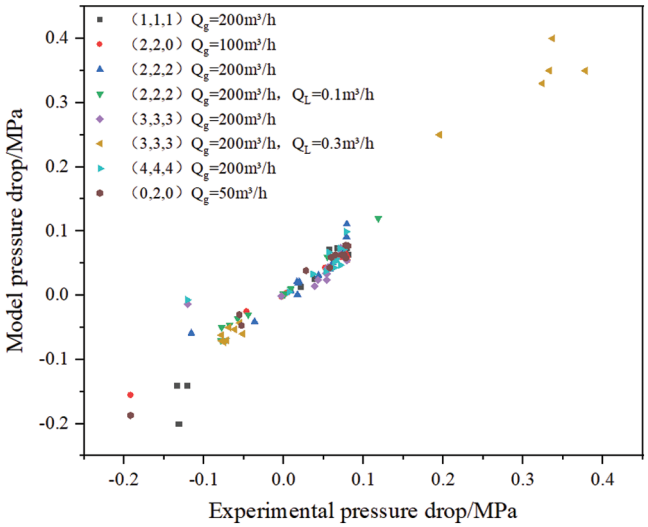


**Figure 16:** Pressure drop comparison chart

### *3.3 Comparative Analysis of Models*

When there are n perforating structures in the pipeline, as shown in Fig. 15, we can establish the following physical model:

In Su's model, it is considered that:

$$\Delta P = \Delta P_{acc} + \Delta P_{wall} + \Delta P_{perf} + \Delta P_{Mix} \tag{5}$$

$$\Delta P_{wall,i} = f_i \frac{\Delta L}{D} \frac{\rho v_i^2}{2} \tag{6}$$

$$f_i = \left\{ -1.8 \log[\frac{6.9}{\mathrm{Re}_i} + \left(\frac{\varepsilon}{3.7D}\right)^{1.11}] \right\}^{-2} \tag{7}$$

Combined with the physical model mentioned in reference [1], it can be concluded that there are:

$$\Delta P = \rho_m (2nv_{m1}v_p \frac{d^2}{D^2} + n^2 v_p^2 \frac{d^4}{D^4}) + \sum_{i=1}^{n} f_i \frac{\Delta L}{D} \frac{\rho v_{mi}^2}{2} + \frac{F_{Mix}}{A} \tag{8}$$

By comparing the results of Eq. (8) with the experimental data, it can be found that the maximum average relative error of pressure drop calculation is 18.8%.

It can be seen from Fig. 16 found that the most error of pressure calculation occurs between the first perforation section and the second perforation section under the opening modes (1,1,1), (2,2,2), (3,3) and (4,4,4). It can also be proved by the experimental data that the change amplitude of pressure drop in this section is indeed higher than that in other parts of the pipe. With the increase of the number of openings, the distribution of pressure drop tends to be stable, but the influence on the downstream of a cluster is not obvious, so it can be explained that the interference between clusters should be considered in the calculation of pressure drop at this point. With the increase of liquid flow, the accuracy of pressure drop calculation in the wellbore is improved. With the increase of perforation number and fluid volume, the pressure drop in the perforated section in the wellbore will increase significantly.

## 4 Conclusion and Prospect

Through the consideration of single gas phase flow and gas-liquid two-phase flow, the pressure distribution in the wellbore under different conditions was studied. The main conclusions are as follows:

1. With the increase of the perforation air flow, the pressure near the perforation clusters also increases. When the number of clusters opened by the perforation increases, the pressure in the wellbore will obviously increase with the perforation changes. When the three clusters of perforations begin to take in air, the pressure in the wellbore changes significantly near the clusters of perforations. The larger the gas volume, the pressure at each point in the wellbore increases. The variation trend of pressure in the wellbore is the same under different opening methods.
2. When the perforation inflow is single-phase or two-phase, there exists: (n, n, n) uniform opening method and (a, b, c) non-uniform opening method, the overall pressure change is smaller. As the number of perforations develops into a uniform opening method, the wellbore pressure changes tend to stabilize. In other areas of the wellbore, the inlet air pressure of 200 $m^3/h$ or less has no significant effect on the pressure in the wellbore.
3. When the liquid holdup in the wellbore is less than 50% and the perforating air intake is more than 200 $m^3/h$, the pressure in the wellbore increases obviously with the continuous increase of gas volume. When the liquid holdup is more than 50%, the pressure only fluctuates greatly near the first perforating cluster.
4. The proposed pressure drop calculation model is in good agreement with the experimental data, and the average relative error of the pressure drop calculation under the selected conditions is controlled within 20%.

Due to the limitations of the indoor experiment, it is necessary to combine the experimental results with the actual situation in the field:

1. Air-water simulation of the flow state of natural gas bottom fluid in horizontal gas wells, due to the influence of physical property differences on the accuracy of the prediction model, field data should also be used for evaluation.
2. The detailed description of the flow field and pressure in the wellbore of the experimental device needs to be further studied with the help of infrared camera, distributed pressure sensor and other technologies.
3. It is necessary to consider more factors such as perforating aperture, fluid medium type, perforating distribution density and perforating section length to analyze the pressure change in horizontal gas well.

**Acknowledgement:** The authors gratefully expressed their thanks for the financial support for these researches from the National Major Scientific and Technological Special Project (2016ZX05046004-002), Foundation of the Educational Commission of Hubei Province of China (No. Q20191310), National Natural Science Foundation of China (Grant No. 61572084).

**Funding Statement:** This work was supported by the National Major Scientific and Technological Special Project (2016ZX05056004-002), Foundation of the Educational Commission of Hubei Province of China (No. Q20191310), National Natural Science Foundation of China (Grant No. 61572084).

**Conflicts of Interest:** The authors declare that they have no conflicts of interest to report regarding the present study.

## References


1. Wang, J. Y., Sun, J., Liu, D. H., Zhu, X. (2019). Production capacity evaluation of horizontal shale gas wells in fuling district. *Fluid Dynamics & Materials Processing, 15(5),* 613–625.
2. Wang, J. F. (2015). *Study on the flow law of variable mass flow in horizontal wellbore with porous injection*. China University of Petroleum (East China), Qingdao, China.
3. Feng, X. Y., Luo, W., Lei, Y., Su, Y., Fang, Z. (2020). Study on dynamic prediction of two-phase pipe flow in inclined wellbore with middle and high yield. *Fluid Dynamics & Materials Processing, 16(2),* 339–358.
4. Liu, X. P. (1998). A new model for calculating steady-state productivity of horizontal wells in gas reservoirs. *Natural Gas Industry, 18(1),* 37–40.
5. Sun, F. J., Han, S. G., Cheng, L. S., Li, X. S. (2005). Coupling model of seepage and horizontal wellbore pipe flow in fractured horizontal well of low permeability gas reservoir. *Journal of Southwestern Petroleum Institute, 27(1),* 32–36.
6. Dongkwon, H., Sunil, K. (2020). Development and application of a production data analysis model for a shale gas production well. *Fluid Dynamics & Materials Processing, 16(3),* 411–424.
7. Dikken, B. J. (1990). Pressure drop in horizontal wells and its effect on production performance. *Journal of Petroleum Technology, 42(11),* 1426–1433.
8. Islam, M. R., Chakma, A. (1990). Comprehensive physical and numerical modeling of a horizontal well. *SPE 20627. Proceedings of the SPE Annual Conference and Exhibition,* New Orleans, LA, USA.
9. Su, Z., Gudmundsson, J. S. (1994). Pressure drop in perforated pipes: Experiments and analysis. *SPE 28800. SPE Asia Pacific Oil & Gas Conference,* Melbourne, Australia.
10. Ouyang, L. B., Aziz, K. (1996). General wellbore flow model for horizontal, vertical, and slanted well completion. *SPE 36608. SPE Annual Technical Conference and Exhibition,* Denver, CO, USA.
11. Zhou, S. T., Zhang, Q., Li, M. Z., Wang, W. Y. (1998). Experimental study on variable mass fluid flow in horizontal wells. *Journal of the University of Petroleum, China, 22(5),* 53–55.
12. Zhou, S. T., Zhang, Q., Li, M. (2002). The advances on the variable mass flow in horizontal wells. *Advances in Mechanics, 32(1),* 119–127.
13. Wang, Z. M., Xiao, J. N., Wang, X. Q. (2011). Experimental study for pressure drop of variable mass flow in horizontal well. *Journal of Experiments in Fluid Mechanics, 25(5),* 26–29.
14. Wei, J. G., Wang, X., Chen, H., Zhang, Q. (2013). Experiment of complex flow in full size horizontal wells with perforated completion. *Petroleum Exploration & Development, 40(2),* 220–225.
15. Zhao, X. (2016). Research on variable density perforating technology in horizontal well. *Well Logging Technology, 40(1),* 122–126.
16. Wen, J., Yang, M., Qi, W. L., Wang, J. (2018). Experimental analysis and numerical simulation of variable mass flow in horizontal wellbore. *International Journal of Heat and Technology, 36(1),* 309–318.
17. Zhang, X., Jiang, Z., Liao, R., Shi, B. Wu, L. et al. (2020). Study on temperature distribution of perforated horizontal wellbore. *Journal of Thermal Sciences, 29(1),* 194–205. DOI 10.1007/s11630-019-1247-9.